Structural Induced Control of Energy Transfer within Zn(II)−Porphyrin Dendrimers

Jane Larsen,[†,§] Ben Brüggemann,[†,⊥] Tony Khoury,[‡] Joseph Sly,[‡,#] Maxwell J. Crossley,[‡] Villy Sundström,*[,†] and Eva Åkesson[†]

Department of Chemical Physics, Lund University, Box 124, SE-221 00 Lund, Sweden, and School of Chemistry, The University of Sydney, NSW 2006, Australia

Received: January 22, 2007; In Final Form: August 5, 2007

We report on a study of singlet−singlet annihilation kinetics in a series of Zn(II)−porphyrin-appended dendrimers, where the energy transfer efficiency is significantly improved by extending the molecular chain that connects the light-harvesting chromophores to the dendrimeric backbone with one additional carbon. For the largest dendrimer having 64 Zn(II)−porphyrins, only ∼10% of the excitation intensity is needed in order to observe the same extent of annihilation in the dendrimers with the additional carbon in the connecting chain as compared to those without. Complete annihilation, until only one chromophore remains excited, now occurs within subunits of seven chromophores, when half of the chromophores are excited. The improvement of the annihilation efficiency in the largest dendrimer with 64 porphyrins can be explained by the presence of a the two-step delayed annihilation process, involving energy hopping from excited to nonexcited chromophores prior to annihilation. In the smallest dendrimer with only four chromophores, delayed annihilation is not present, since the direct annihilation process is more efficient than the two-step delayed annihilation process. As the dendrimer size increases and the chances of originally exciting two neighboring chromophores decreases, the delayed annihilation process becomes more visible. The additional carbon, added to the connecting chain, results in more favorable chromophore distances and orientations for energy hopping. Hence, the improved energy transfer properties makes the Zn(II)−porphyrin-appended dendrimers with the additional carbon promising candidates as light-harvesting antennas for artificial photosynthesis.

1. Introduction

The molecular group of dendrimers has attracted a lot of attention in recent years due to, among others, their applications in guest−host chemistry,[1,2] optical data storage,[3,4] medical applications,[5] biology,[6−11] catalytic chemistry,[12] analytical chemistry,[13] and environmental chemistry.[14,15] Dendrimers have been proposed for use as light-harvesting antennas in artificial photosynthesis due to their large cross section for light absorption and their capability of directional energy transfer (ET) within the dendrimers.[13−49] The ET mechanism is often a result of dipole−dipole interactions between the chromophores and can be well described by Förster ET theory[50,51] as shown previously for various types of dendrimers.[36−49]

In the porphyrin-appended dendrimers studied in this article, all the Zn(II)−porphyrin chromophores are identical and the ET is consequently not associated with any spectral changes. Nevertheless, information on the ET can be obtained by means of either time-resolved anisotropy[52] or intensity-dependent transient absorption measurements (singlet−singlet annihilation)[53,54] as demonstrated previously. If the chromophores interact strongly, an anisotropy signal can contain contributions from energy relaxation between exciton states. However, as shown previously,[52−54] the Zn(II)−porphyrins in these dendrimers do not interact strongly, and exciton states will not interfere with the anisotropy signal. Contribution from rotational motion of the chromophores in the dendrimers will on the other hand mix with the ET signal. At room temperature these two contributions cannot be accurately separated. Previously it was shown that the individual chromophores rotate almost as freely as the monomer,[52] which means that a large contribution from rotational motion is present in all the dendrimers independent of molecular size.

Singlet−singlet annihilation is very sensitive to ET between the excited states and furthermore not influenced by rotational motion to the same extent as the anisotropy. Consequently, this experimental approach was used in this study. The method accounts for ET between excited states and give thereby clear—though indirect—information about the general communication and ET between excited and nonexcited chromophores in the system. Due to mainly the difference in the spectral overlap integral required in singlet−singlet annihilation between two excited chromophores compared to energy hopping between an excited and a nonexcited chromophore, the two ET times will differ. For the dendrimers studied in this article, it was shown previously that the annihilation ET time is approximately 5 times faster than the ET hopping time.[53]

In an earlier singlet−singlet annihilation study, ET between all the chromophores was found to occur in the smallest dendrimer containing four chromophores with reasonably good efficiency.[53] A second study showed that by changing the solvent from the polar tetrahydrofuran (THF) to the nonpolar 3-methylpentane (3MP), the ET rates were increased by more than 25%.[54] The increase in transfer rate was found to be directly

* Corresponding author. E-mail: Villy.Sundstrom@chemphys.lu.se.
† Lund University.
‡ The University of Sydney.
§ Current address: Center for Oxygen Microscopy and Imaging, Department of Chemistry, University of Aarhus, DK-8000 Århus, Denmark.
⊥ Current address: Department of Physics, Humboldt University at Berlin, Newtonstr. 15, 12489 Berlin, Germany.
Current address: IBM Almaden Research Center, 650 Harry Rd, San Jose, CA 95120.

10.1021/jp070545g CCC: $37.00
Published on Web 10/03/2007

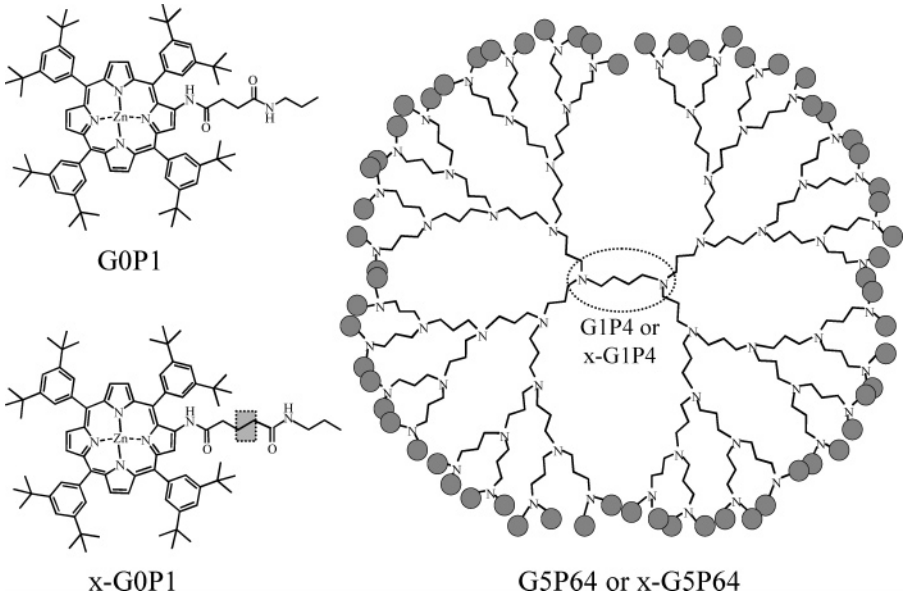

Figure 1. Structure of G*n*P*r* and x-G*n*P*r*, the latter where the chain connecting the Zn(II)−porphyrins to the dendrimeric backbone has been extended by an additional carbon.

related to a decrease in the hydrodynamic radius upon changing solvent. For the smallest generation dendrimer, the ET efficiency was completely optimized as an effect of the enhanced ET rates. However, in the largest generation dendrimer with 64 Zn(II)−porphyrins, further enhancement of the ET was still possible, since complete annihilation was only observed within a subunit of four chromophores. The present study shows how the ET efficiency in the larger generation dendrimers can be improved significantly by a minor modification of the chain connecting the Zn(II)−porphyrin chromophores to the dendrimeric backbone.

2. Materials and Methods

The synthesis and purification of the compounds have been described elsewhere.[55,56] Before use, the compounds were dissolved in 3MP purchased from Aldrich and used without further purification. The optical density at 430 nm was 0.1 mm^{-1} and less than 0.01 mm^{-1} in the steady-state absorption and fluorescence experiments, respectively. In the time-resolved experiments, the optical density at 400 nm varied between 0.4 and 1.0 mm^{-1}, giving concentrations below 10^{-4} M.[52,57] Fresh samples were made prior to each measurement in order to avoid degradation of the samples. Absorption spectra measured before and after each measurement showed no sign of degradation.

Steady-state absorption and fluorescence spectra were measured on a UV−vis diode array spectrophotometer and a Spex Fluorolog II, respectively. The fluorescence spectra were detected with a photomultiplier tube (PMT) using a spectral resolution of 0.5 nm. The spectra were afterward corrected for the wavelength-dependent PMT sensitivity. The femtosecond transient absorption setup based on an amplified Ti:Sapphire laser is described in detail elsewhere.[53] By frequency doubling a part of the fundamental, the 400 nm pump light was acquired. In our previous studies, the transient absorption spectrum of the Zn(II)−porphyrin monomer measured from 450 to 730 nm showed that 490 nm is a suitable wavelength for probing the excited-state dynamics.[53] By focusing the other part of the fundamental into a 5 mm sapphire plate, a white light continuum was generated from where the 490 nm probe light was selected. The polarization of the excitation light was set to 54.7° (magic angle) with respect to the polarization of the probe light using a Berek polarization compensator. In order to vary the intensity of the excitation light from 3×10^{14} to 7×10^{16} photons/cm^2 per pulse, neutral density filters were inserted before the sample. A 2 mm rotational quartz cuvette was used in the experiments yielding a time resolution of ~200 fs.

3. Structural and Spectral Characteristics of the Zn(II)−Porphyrin Dendrimers

The Zn(II)−porphyrin-appended polypropylenimine dendrimers, illustrated in Figure 1, are derived from a single-bonded nitrogen and carbon backbone onto which Zn(II)−porphyrins have been attached at the end of each dendrimer arm. Two different connecting chains are used to attach the Zn(II)−porphyrins to the dendrimeric backbone: the "original" dendrimers (G*n*P*r*, where n = generation number and r = number of Zn(II)−porphyrins) studied previously,[52−54] and the "new" dendrimers (x-G*n*P*r*) studied in this article. In x-G*n*P*r*, one additional carbon has been added to the connecting chain. By systematic expansion of the dendrimeric backbone, five generations of dendrimers are created, ranging in size from the smallest generation dendrimer with 4 Zn(II)−porphyrins (G1P4/x-G1P4) to the largest generation with 64 Zn(II)−porphyrins (G5P64/x-G5P64). The three-dimensional structure of the fifth-generation dendrimer resembles a sphere with the Zn(II)−porphyrins situated on the surface, since the size of the bulky end-groups prevents back-folding.[41,55] The dotted circle inside the fifth-generation dendrimer (see Figure 1) marks the position of the Zn(II)−porphyrins in the smallest generation dendrimer (G1P4/x-G1P4).

Normalized steady-state absorption and fluorescence spectra of G1P4 and x-G1P4 are displayed in Figure 2. Only minor variations are observed in the normalized spectra depending on the generation number, and G1P4 and x-G1P4 are therefore representative examples of the G*n*P*r* and x-G*n*P*r* dendrimer absorption spectra, respectively. The strongly absorbing Soret band is centered at 430 nm ($S_2 \leftarrow S_0$), and the two much weaker Q-bands are present around 555 and 600 nm, where the splitting is due to absorption to the first and the zero vibrational state ($S_1[1] \leftarrow S_0[0]$ and $S_1[0] \leftarrow S_0[0]$, respectively). Since there are only negligible differences between the absorption spectra of the monomer (G0P1/x-G0P1) and the dendrimers, strong

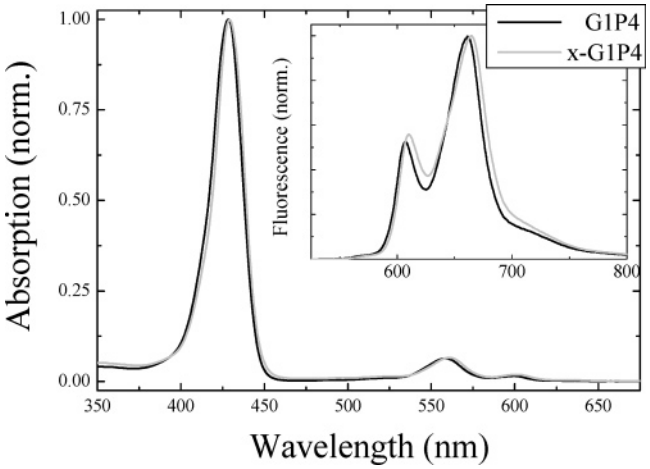

Figure 2. Steady-state absorption spectra of G*n*P*r* exemplified by G1P4 (black line) and x-G*n*P*r* exemplified by x-G1P4 (gray line) are shown in the graph. The inset displays the emission spectra of the two different dendrimer types.

interactions between the Zn(II)−porphyrins within the same dendrimer are not present.[52−54] Upon excitation into the Soret band (S_2) internal conversion (IC) to the Q-band (S_1) occurs in less than 1 ps,[53] from where two fluorescence bands with maxima at 600 nm ($S_1[0] \rightarrow S_0[0]$) and 655 nm ($S_1[0] \rightarrow S_0[1]$) can be observed. The fluorescence spectra of G1P4 and x-G1P4 are shown in the inset of Figure 2. Again, only minor differences are observed depending on the generation number. In addition to the Q-band fluorescence, there is an efficient intersystem crossing (ISC) from the S_1 state to the triplet manifold, from where phosphorescence can be observed at wavelengths above 800 nm.[58]

The transient absorption spectra of both G*n*P*r* and x-G*n*P*r* recorded in the spectral range from 450 to 730 nm 1 ps after excitation exhibit similar features independently of the generation number (data not shown here). At our chosen probe wavelength (490 nm), it has been shown previously that only S_1 and T_1 excited-state absorption contribute to the signal.[53] Contributions from both ground state bleach and stimulated emission signals can thus safely be ignored in the further analysis.

4. Singlet−Singlet Annihilation Theory

At low excitation intensity, only one chromophore is excited within the same dendrimer. Energy hopping can then occur from the excited chromophore to a nonexcited chromophore. The time scale for the energy hopping between the two nearest neighboring chromophores separated by approximately 2 nm is ∼100 ps as calculated previously[52] using Förster ET theory. When the excitation intensity is increased, more than one Zn(II)−porphyrin chromophore can be excited simultaneously, which facilitates interactions between the excited chromophores observed as singlet−singlet annihilation. Energy is transferred between two excited Zn(II)−porphyrins, de-exciting one of the chromophores to the ground state while exciting the other to a higher lying state, from where it will relax back to the lowest excited state through fast IC.

$$S_1 + S_1 \xrightarrow{\text{ET}} S_0 + S_n \xrightarrow{\text{fast IC}} S_0 + S_1 \qquad (1)$$

The population of the S_1 state is reduced as a result of the singlet−singlet annihilation process, which will be observed as a decay of the transient absorption kinetics at 490 nm. Contributions from singlet−triplet and triplet−triplet annihilation can be ignored, since the ISC to the triplet manifold is slow compared to the observed time window.[58] In order to analyze the singlet−singlet annihilation kinetics, a rate equation model based on the procedure described by van Amerongen et al.[59] was developed in a previous publication.[53] Application of the model reveals that at least two annihilation processes are present, described by a fast and a slow annihilation rate constant. The two annihilation rates represent the minimum number of rate constants required in order to describe the annihilation kinetics and are thus part of a broader distribution of rates.

In the rate equation model, the number of excited chromophores, which annihilate with the fast (k_f) or the slow rate constant (k_s) and the number of excited chromophores not involved in annihilation, are described separately. If more than two chromophores are excited simultaneously, the chromophore still excited after one annihilation step can annihilate again with a third excited chromophore. This process is referred to as sequential annihilation and has previously been included in the annihilation amplitudes.[53,54] However, as the sequential annihilation becomes more efficient and involves multiple steps, it becomes essential to separate the contributions from chromophores annihilating once, twice, or more times. In this study, we have chosen to describe the sequential annihilation within a unit of four chromophores, where one, two, three, or four chromophores can be excited simultaneously. The model can be extended to include contributions from sequential annihilation within units of five or more excited chromophores as could potentially occur in the largest dendrimer. However, expanding the model further is not a trivial task and will therefore not be pursued here. The amplitude of the set of excited chromophores annihilating three times (E^{3M}) either by the M = fast (f) or the M = slow (s) annihilation rate are described by eq 2, and those that annihilate twice (E^{2M}) and once (E^{1M}) are described by eqs 3 and 4, respectively.

$$\frac{dE^{3M}}{dt} = -6k_M E^{3M}(t) \qquad (2)$$

$$\frac{dE^{2M}}{dt} = -3k_M E^{2M}(t) + 6k_M E^{3M}(t) \qquad (3)$$

and

$$\frac{dE^{1M}}{dt} = -k_M E^{1M}(t) + 3k_M E^{2M}(t) \qquad (4)$$

with the initial amplitudes $E^{xM}(t = 0) = E_0^{xM}$ for $x = 1$, 2, and 3. The integers before the rate constants represent the number of annihilating pathways. Mixed contributions from chromophores that annihilate first with a fast/slow and second by a slow/fast annihilation rate are for reasons of simplicity not included as separate contributions in the model. The number of excited chromophores that will not annihilate (S) are described as

$$\frac{dS}{dt} = -kS(t) + k_f E^{1f}(t) + k_s E^{1s}(t) \qquad (5)$$

where the decay rate of the S_1 state (k) is a sum of the ISC rate (k_{isc}), the radiative decay (k_{rad}), and the rate of IC to the ground state (k_{IC}). The chromophores that relax to the triplet state (T) are given as

$$\frac{dT}{dt} = qkS(t) - k_T T(t) \qquad (6)$$

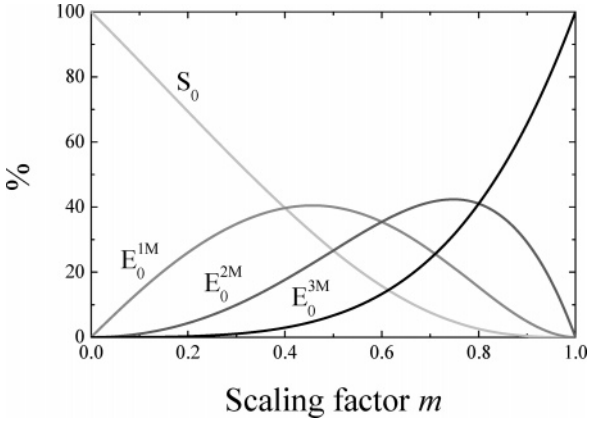

Figure 3. Amplitude distribution as a function of the scaling factor *m* giving the excitation probability.

where q is the ISC quantum yield (hence $k_{ISC} = qk$). Because the decay of the triplet state $k_T \ll k_{ISC}$ it is consequently set to zero. In the spectral range where only excited-state S_1 and T_1 absorption is observed, the transient absorption kinetics can be expressed by eq 7:

$$\Delta A(t) = S(t) + 2[E^{1s}(t) + E^{1f}(t)] + 3[E^{2f}(t) + E^{2s}(t)] + 4[E^{3f}(t) + E^{3s}(t)] + pT(t) \quad (7)$$

where E^{1M}, E^{2M}, and E^{3M} are counted two, three, and four times, respectively, since they represent multiple excitations, and p is the ratio between the extinction coefficient of the singlet and the triplet excited state. Within a unit of four Zn(II)−porphyrins, there will be a statistical distribution between the concentration of one, two, three, and four excited chromophores. This places some restrictions on the ratio between the different amplitudes S_0, E_0^{1M}, E_0^{2M}, and E_0^{3M}. The scaling factor "m" is defined as $0 \leq m \leq 1$ and gives the probability of exciting a chromophore. Hence, at low excitation intensity, m is close to zero and at high excitation intensity m is approaching unity. For P_0^f and $P_0^s = 1 - P_0^f$ being the fraction of fast and slow annihilating chromophores, respectively, the amplitudes S_0, E_0^{1M}, E_0^{2M}, and E_0^{3M} can be written as

$$S_0 = 4m(1-m)^3 \quad (8)$$

$$E_0^{1M} = 6m^2(1-m)^2P_0^M \quad (9)$$

$$E_0^{2M} = 4m^3(1-m)P_0^M \quad (10)$$

and

$$E_0^{3M} = m^4P_0^M \quad (11)$$

where the integers count the number of possibilities of exciting one, two, three, or four chromophores. In this manor, the statistical distribution is ensured. M = f or M = s again represents the fast and the slow annihilation process, respectively. The amplitude distribution between the concentration of one, two, three, and four excited chromophores relative to the sum of all excitations are plotted in percent as a function of m in Figure 3. Solving eqs 2−6 and utilizing the restrictions given in eqs 8−11, yields a solution to eq 7 given by

$$\Delta A = A_0 + A_k \exp(-kt) + A_{k_{1f}} \exp(-k_f t) + A_{k_{1s}} \exp(-k_s t) + A_{k_{2f}} \exp(-3k_f t) + A_{k_{2s}} \exp(-3k_s t) + A_{k_{3f}} \exp(-6k_f t) + A_{k_{3s}} \exp(-6k_s t) \quad (12)$$

where

$$A_0 = qpm[2(1-m)^2(2+m) + m^2(4-3m)] \quad (13)$$

$$A_k = 2(1-qp)\left\{P_0^f \frac{k_f}{k_f - k} m\left[(2+m)(1-m)^2 + \frac{3k_f}{3k_f - k} m^2\left(2 - 2m + 3m\frac{k}{k-6k_f}\right)\right] + P_0^s \frac{k_s}{k_s - k} m\left[(2+m)(1-m)^2 + \frac{3k_s}{3k_s - k} m^2\left(2 - 2m + 3m\frac{k}{k-6k_s}\right)\right]\right\} \quad (14)$$

$$A_{k_{1M}} = m^2\left(6 - 6m + \frac{9}{5}m^2\right)P_0^M\left[1 + (1-qp)\frac{k_M}{k_M - k}\right] \quad (15)$$

$$A_{k_{2M}} = m^3(2-m)P_0^M\left[1 + (1-qp)\frac{k}{3k_M - k}\right] \quad (16)$$

and

$$A_{k_{3M}} = \frac{1}{5}m^4P_0^M\left[1 + (1-qp)\frac{k}{k - 6k_M}\right] \quad (17)$$

An advantage in applying the restriction to the annihilation rate equations is that it reduces the number of unknowns to only count p, q, m, P_0^s, k, k_f, and k_s. For a similar Zn(II)−porphyrin monomer, $k^{-1} = 2700$ ps and $q = 0.84$ has been reported.[58] These two values will be used in the further analysis, thereby reducing the number of unknowns to only five.

5. Results

The intensity-dependent kinetics measured at 490 nm for x-G1P4 and x-G5P64 dissolved in 3MP are shown in the left and the right-hand side of Figure 4, respectively. Next to the kinetics, the excitation intensity of $x \times 10^{14}$ photons/cm^2 per pulse is listed. In both graphs, the kinetics recorded at high intensity for the symmetric monomer without a connecting chain is shown. The monomer kinetic displays a slow rise due to ISC to the triplet manifold, since the extinction coefficient of the $T_1 \rightarrow T_n$ transition is higher than the extinction coefficient of the $S_1 \rightarrow S_n$ transition. No intensity dependence is observed in the monomer kinetics in contrast to the dendrimer kinetics where a strong intensity dependence is present. Since, the intensity dependence in the dendrimers is not associated with any process within the individual Zn(II)−porphyrins, we assign it to exciton−exciton annihilation. The ISC rate is relatively slow ($k_{ISC}^{-1} \approx 3200$ ps[58]) and the concentration of singlet excited states is therefore dominant compared to the concentration of triplet states. Accumulation of triplet states does not occur, as a rotational cuvette is used in the measurements. Contribution from annihilation processes involving triplet states can consequently be neglected. Thus, the exciton−exciton annihilation process is assigned to singlet−singlet annihilation.

The intensity-dependent kinetics are analyzed using the rate equation model derived in the previous section. For the

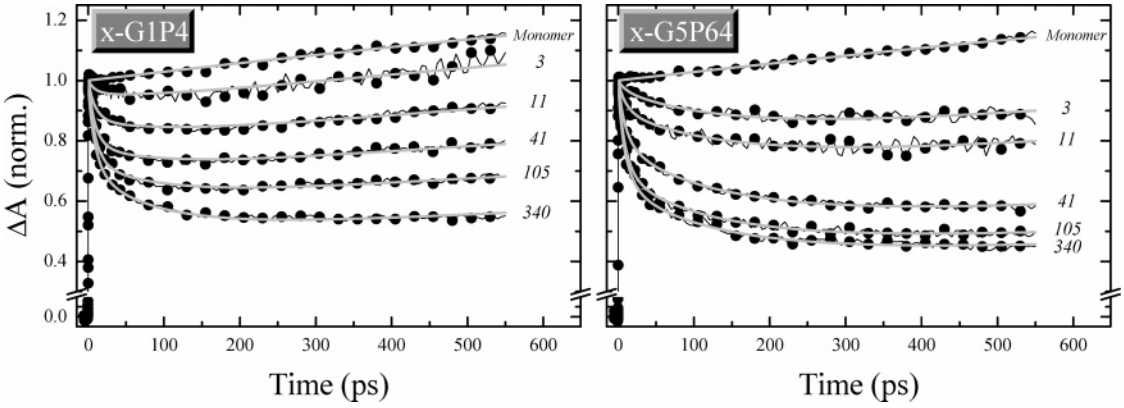

Figure 4. Singlet−singlet annihilation kinetics observed in x-G1P4 and x-G5P64 are shown in the left-hand and the right-hand graphs, respectively. Next to the data traces, the excitation intensity is listed given in units of $x \times 10^{14}$ photons/cm^2 per pulse. The solid gray lines are fits of the data obtained using the rate equation model described in the text.

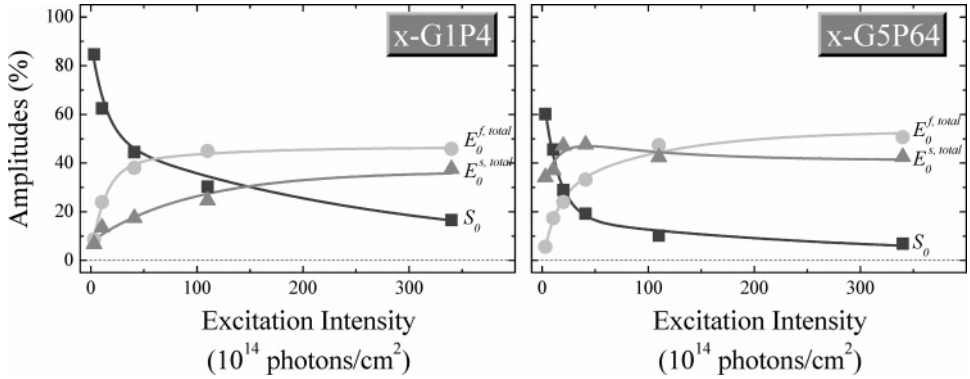

Figure 5. Amplitude of the chromophores not involved in annihilation (S_0) and the total amplitude of the chromophores involved in the fast and the slow annihilation process ($E_0^{f,total}$ and $E_0^{s,total}$, respectively) are plotted as a function of the excitation intensity for x-G1P4 (left-hand graph) and x-G5P64 (right-hand graph). The lines drawn behind the points are double-exponential fits meant only as guidance for the eye.

monomer kinetics, one has only to take into account eqs 5 and 6 using $E_0^{1f} = E_0^{1s} = 0$, as annihilation is absent. This reduces the annihilation rate model significantly. When applying the previously reported value for the S_1 state lifetime ($k^{-1} =$ 2700 ps) and the ISC yield ($q = 0.84$) for a similar compound,[58] only the ratio between the extinction coefficients of the triplet and the singlet state (p) is an unknown parameter in the rate equation model describing the monomer kinetics. Therefore, from the monomer kinetics $p = 2.12$ can be obtained and is used in the further analysis of the dendrimer annihilation kinetics. The solid lines in Figure 4 superimposed on the measurements are fits of the data using eqs 12−17. The dendrimer intensity-dependent kinetics are analyzed globally in order to acquire the same annihilation rates at all intensities within one dendrimer. For x-G*n*P*r* with the extended connecting chain, the fast annihilation rate k_f^{-1} (x-G*n*P*r*) = 10 ± 5 ps is the same as observed previously in G*n*P*r*.[54] However, the slow annihilation rate differs depending on the generation number yielding values of k_s^{-1} (x-G1P4) = 100 ± 30 ps and k_s^{-1} (x-G5P64) = 165 ± 30 ps, compared to k_s^{-1} (G*n*P*r*) = 145 ± 30 ps.

For all the dendrimers, a saturation level is reached, at which stage further increase of the excitation intensity does not induce additional annihilation. The saturation level is calculated as the difference between the transient absorption data of the monomer kinetics and the dendrimers at 550 ps, both measured at high intensity. In G*n*P*r*, the saturation level has previously been reported to be the same independent of the dendrimer size.[53,54] For x-G*n*P*r*, a lower saturation level is observed in x-G5P64 compared to x-G1P4 as can be seen in Figure 4. Hence, annihilation becomes more efficient the larger x-G*n*P*r* is. Table 1 lists the saturation level and the annihilation rate constants for both G*n*P*r* and x-G*n*P*r*, and also includes the values for the second-generation dendrimers, G2P8 and x-G2P8.

TABLE 1: Values of the Saturation Level and the Annihilation Rates

	saturation level (%)[a]	k_f^{-1} (ps)	k_s^{-1} (ps)
G1P4	47	10 ± 5	145 ± 30
G2P8	46	10 ± 5	145 ± 30
G5P64	47	10 ± 5	145 ± 30
x-G1P4	41	10 ± 5	100 ± 30
x-G2P8	37	10 ± 5	150 ± 30
x-G5P64	30	10 ± 5	165 ± 30

[a] The saturation level is given as the difference between the monomer kinetics and the dendrimer kinetics at 550 ps.

The values of S_0, $E_0^{f,total}$ (= $2E_0^{1f} + 3E_0^{2f} + 4E_0^{3f}$), and $E_0^{s,total}$ (= $2E_0^{1s} + 3E_0^{2s} + 4E_0^{3s}$) obtained from the fits of the x-G1P4 and x-G5P64 data are plotted in Figure 5 as a function of the excitation intensity. It can be seen that the amount of excited Zn(II)−porphyrins not involved in annihilation (S_0) is somewhat larger in x-G1P4 than in x-G5P64. The total number of chromophores involved in either the fast ($E_0^{f,total}$) or the slow ($E_0^{s,total}$) annihilation processes includes contributions from one, two, and three annihilation processes. Figure 5 shows that the number of chromophores annihilating with the fast rate constant increases as a function of the excitation intensity following the same trend, independent of dendrimer size. However, the number of chromophores annihilating with the slow rate constant

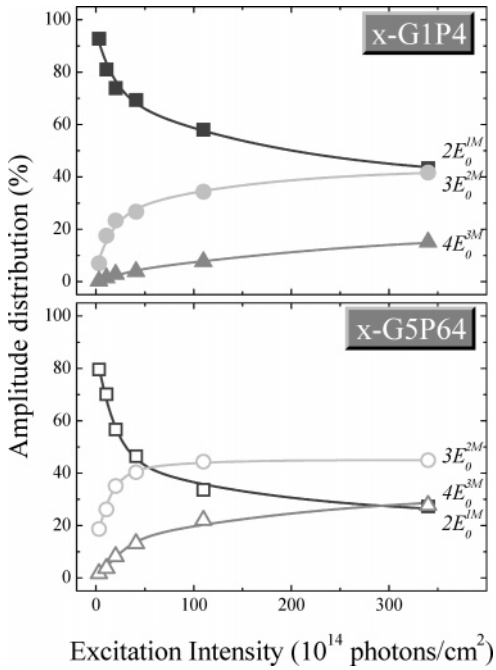

Figure 6. Distributions of the amplitudes describing annihilation within a unit of four chromophores, where two ($2E_0^{1M}$), three ($3E_0^{2M}$), or four ($4E_0^{3M}$) of them are excited simultaneously, are shown in the top graph for x-G1P4 and in the bottom graph for x-G5P64 as a function of the excitation intensity. The same picture is obtained for both M = f and M = s. Behind the symbols, double-exponential fits are drawn only as guidance for the eye.

is strongly dependent on the size of the dendrimer. In x-G1P4, $E_0^{s,total}$ increases as a function of the excitation intensity, whereas it is more or less independent of excitation intensity in x-G5P64.

The scaling factor m is higher in x-G5P64 than in x-G1P4, when comparing the values obtained at the same excitation intensity. As a consequence, the distribution of Zn(II)−porphyrins annihilating one, two, or three times recorded at the same excitation intensity is different in x-G1P4 and x-G5P64, as illustrated in Figure 6. At the saturation level (highest excitation intensity) in x-G1P4, the number of chromophores involved in one and two annihilation processes ($2E_0^{1M}$ and $3E_0^{2M}$, respectively) is the same, which corresponds to 50% of the chromophores being excited on average. However, in x-G5P64 there is a higher percentage of the chromophores involved in two or three annihilation processes ($3E_0^{2M}$ and $4E_0^{3M}$, respectively) compared to x-G1P4. To describe the annihilation process in x-G5P64 more accurately, contributions from chromophores involved in four, five, six, etc. annihilation processes should in principle be included. However, this is not a trivial task; the assumption that all chromophores can annihilate with one another is not valid for units with more than four chromophores. The amplitude of $4E_0^{3M}$ therefore includes a small contribution from annihilation within units of five and six chromophores also.

6. Discussion

6.A. Annihilation within G*n*P*r* Compared to x-G*n*P*r*. Annihilation is clearly more efficient in x-G*n*P*r* compared to G*n*P*r* as seen in Figure 7, where the annihilation kinetics measured at the same excitation intensities are compared for the two types of dendrimers. It is apparent from the figure that this effect becomes more pronounced the higher the dendrimer generation. The fast annihilation rate constant is independent of dendrimer generation and type (see Table 1). This implies that the distance between the closest neighboring Zn(II)−porphyrins (the main factor influencing the fast annihilation rate) does not change much depending on dendrimer generation or type.

The small differences observed in the annihilation kinetics of G1P4 and x-G1P4 can be explained by the increase of the slow annihilation rate from k_s^{-1} (G1P4) = 145 ± 30 ps to k_s^{-1} (x-G1P4) = 100 ± 30 ps. Conversely, in the largest dendrimer with 64 Zn(II)−porphyrins there is a dramatic enhancement of the annihilation efficiency in x-G*n*P*r* compared to G*n*P*r* (see Figure 7): the same degree of annihilation requires 10 times lower excitation intensity in x-G5P64 compared to G5P64. For G1P4/x-G1P4, the difference in annihilation efficiency is explained by an increase of the slow annihilation rate. In G5P64/x-G5P64, the slow annihilation rate instead decreases slightly. In order to explain why the annihilation is clearly more efficient in x-G5P64 than in G5P64, we need to consider the amplitudes of the fast and the slow annihilation components in the two dendrimers. The amplitude of the fast annihilation component ($E_0^{f,total}$) at a specific excitation intensity varies only to a minor extent depending on the length of the dendrimeric connecting chain. The slow annihilation amplitude is more or less constant at all excitation intensities in x-G5P64, whereas it exhibits

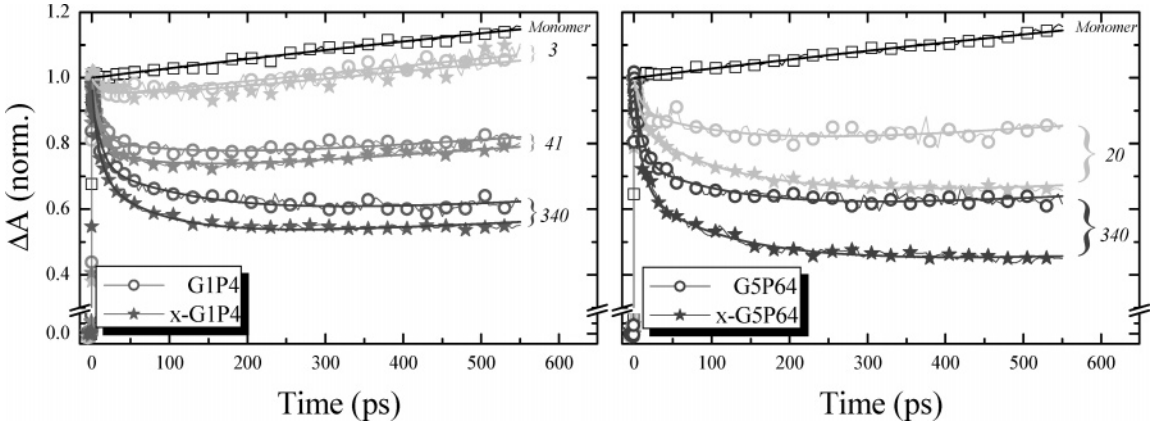

Figure 7. Singlet−singlet annihilation kinetics observed in G*n*P*r* (circles) compared to x-G*n*P*r* (stars) recorded at the same excitation intensities. In the left-hand graph, the kinetics measured in the smallest generation dendrimer are shown, whereas the kinetics measured in the largest are displayed in the right-hand graph. The excitation intensities are listed next to the traces in unit of $x \times 10^{14}$ photons/cm^2 per pulse. For comparison, the monomer kinetic plots are shown in both graphs. The solid lines superimposed on the measurement points are the fits of the data.

significant variation with intensity for G5P64. Hence, compared to G5P64, $E_0^{s,total}$ (x-G5P64) is larger, especially at low excitation intensities. In dendrimers with more than four chromophores, annihilation can occur subsequent to energy hopping between an excited and a nonexcited chromophore. This two-step process, referred to as "delayed annihilation", is not accounted for in the annihilation rate equation model which describes annihilation within a subgroup of four chromophores, all able to annihilate directly with one another. If the chromophores in the larger x-G*n*P*r* dendrimers couple more strongly than in the G*n*P*r* dendrimers, delayed annihilation will become increasingly important. The delayed annihilation process occurs on a time scale longer than the energy hopping time, previously found to be 100 ± 25 ps for energy hopping between two nearest neighboring chromophores.[52] The delayed annihilation process observed in x-G5P64 is, as stated above, not included as a separate contribution in the rate equation model describing annihilation within a subgroup of four chromophores. Therefore, the amplitude related to the slow annihilation process will in x-G5P64 also contain contribution from the delayed annihilation. At higher excitation intensities, more chromophores are excited and the effect of delayed annihilation decreases, since the need of a two-step process in order to observe annihilation becomes smaller when the probability of having two excited chromophores as nearest neighbors from the beginning increases. Consequently, delayed annihilation will predominantly be observed at lower excitation intensities, explaining the almost constant level of $E_0^{s,total}$ in x-G5P64. The huge increase in the annihilation efficiency in x-G5P64 compared to G5P64 can thus be assigned to an increase in the communication between the chromophores, resulting in more effective energy hopping yielding delayed annihilation. A similar effect is not observed in the smallest dendrimers, since all four chromophores can annihilate directly and the two-step delayed annihilation process is thus suppressed by the direct one-step annihilation process.

6.B. Annihilation Efficiency. The saturation level observed in all the measurements provides information on the overall efficiency of the annihilation process, including both sequential and delayed annihilation. Hence, the lower the saturation level, the higher the efficiency. The saturation level (L) obtained when (1) on average 50% of the chromophores within a subunit of y chromophores are excited, and (2) complete annihilation occurs until one excitation remains, is given as

$$L = \frac{\Delta A_{after}}{\Delta A_{before}} = \sum_{x=1}^{y} \frac{y!}{x!(y-x)!}\frac{1}{x} \qquad (18)$$

where x counts the number of excitations within the y chromophores, and ΔA_{before} and ΔA_{after} are the transient absorption signal before and after complete annihilation, respectively. In the smallest dendrimers, the observed saturation level of $L = 47\%$ agrees very well with the situation where $y = 4$ in eq 18. Complete annihilation is thus observed between all the chromophores in x-G1P4. For G*n*P*r* the saturation level was independent of dendrimers size, suggesting that full communication in the larger dendrimers is not present. If complete annihilation occurs in the largest dendrimer with 64 chromophores, a saturation level of 3% should be observed (obtained from eq 18 with $y = 64$). However, complete sequential annihilation is not possible, since the efficient ISC to the triplet manifold will decrease the concentration of excited chromophores in the singlet state before the multiple energy hopping steps (which are needed in order to bring the remaining excited chromophores in close enough proximity to facilitate annihilation) would have time to occur. For x-G5P64, a saturation level of 30% is observed corresponding to a situation where complete annihilation occurs within a subunit of approximately seven chromophores according to eq 18. Hence, complete annihilation in x-G5P64 occurs within a subunit of almost twice the number of Zn(II)−porphyrins as compared to G5P64. As discussed earlier, this improvement in annihilation efficiency is assigned to more pronounced energy hopping in x-G5P64 compared to G5P64 resulting delayed annihilation. Figure 6 shows that sequential annihilation is occurring within a subunit of more than four chromophores in x-G5P64 compared to x-G1P4.

6.C. Additional Carbon. The structural difference between G*n*P*r* and x-G*n*P*r* is very small. Considering the hydrodynamic radius of the dendrimers, one would expect that (1) the hydrodynamic radius increases upon adding an extra carbon and that (2) the smallest dendrimer would be affected to the largest extent. Assuming that the hydrodynamic radius and thereby the chromophore−chromophore distance (R) becomes larger would in turn mean that the energy transfer described by Förster ET theory should become slower.[50,60] The Förster ET rate is given as

$$k_{ET}^{Förster} = \frac{1}{(4\pi\epsilon_0\hbar)^2 c}|\kappa\mu_A\mu_D|^2\Theta R^{-6} \qquad (19)$$

where μ_D and μ_A are the dipole moments of the donor and the acceptor chromophore, respectively, and κ is the dipole−dipole orientation factor. Since the emission spectrum of the donor and the excited-state absorption spectrum of the acceptor are basically identical in both types of dendrimers, the overlap integral (Θ) and the dipole moments (μ_D and μ_A) are independent of the length of the connecting chain. Hence, only changes in the dipole−dipole orientation factor (κ) and/or the chromophore−chromophore distance (R) are expected to alter the Förster ET rate when inserting the additional carbon in the connecting chain. Though the ET time is expected to be most affected by the structural modification in the smallest dendrimer, the data show the opposite trend, and an increase in hydrodynamic radius can consequently not explain the observed increase of the ET efficiency in x-G*n*P*r*. Furthermore, the ET process becomes more efficient and distinct for the bigger dendrimers having an extended connecting chain. It is possible that the dipole−dipole orientation factor could change when the connecting chain is extended, thereby allowing a more favorable orientation of the dipole moments. A change of 20% can account for the increase in ET efficiency, which increases the slow annihilation rate in the smallest dendrimer. A small hint of this improved dipole−dipole orientation (and thereby enhanced coupling between the chromophores) is found when comparing the steady-state spectra, where a small red-shift reminiscent of a slightly stronger coupling between the chromophores is observed in x-G*n*P*r* compared to G*n*P*r*. The increase of the connecting chain might also allow the chromophores to move even more freely or perhaps bend a bit backward, thereby actually reducing the chromophore−chromophore distance instead of increasing it. A small decrease in distance of approximately 6% can also explain the faster annihilation rates observed. We therefore propose that the additional carbon in the connecting chain allows for a larger chromophoric degree of freedom bringing about a larger κ value and/or a smaller value of R.

In x-G5P64, the slow annihilation rate seems to decrease compared to the slow annihilation in x-G1P4 (k_s^{-1} (x-G1P4) = 100 ± 30 ps and k_s^{-1} (x-G5P64) = 165 ± 30 ps). However,

this decrease can be explained by a contribution from delayed annihilation observed only in x-G5P64. If the slow annihilation process could be distinguished from the delayed annihilation process, the slow annihilation in x-G5P64 would most probably be identical to that found in x-G1P4.[53,54]

The addition of one additional carbon in the connecting chain significantly improves the overall ET efficiency in the larger dendrimers, lowering the saturation level from 47% to 30%. This effect is assigned to the presence of delayed annihilation brought about by more effective energy hopping between the chromophores. In the small dendrimers delayed annihilation is not present, since the direct annihilation is faster than the energy hopping mechanism, which precedes the delayed annihilation. However, in the large dendrimers energy hopping may contain several consecutive steps and the energy can be spatially transferred around in the larger dendrimers allowing for delayed annihilation. In order to obtain complete annihilation between all the chromophores in the largest dendrimer, the slow annihilation rate component and the energy hopping needs to be optimized further. This study clearly demonstrates how the energy hopping can be improved by adding one additional carbon to the connecting chain. If the connecting chain is extended with yet another methyl group, further improvement could possibly be obtained.

7. Summary

In this study we have demonstrated how the ET efficiency can be significantly improved by extending the molecular chain that connects the light-harvesting chromophores to the dendrimeric backbone in a series of Zn(II)−porphyrin-appended dendrimers. Only ∼10% of the excitation intensity was needed in order to observe the same degree of annihilation in x-G5P64 as compared to G5P64 without the additional carbon in the connecting chain. Complete annihilation is now obtained within a subunit of seven chromophores in x-G5P64 instead of four chromophores in G5P64 when on average half of the chromophores are excited.

The increased annihilation efficiency in x-G5P64 was shown to be not so much a result of an increase in the annihilation rates but more as a considerable enhancement of the two-step delayed annihilation process subsequent to energy hopping between excited and nonexcited chromophores. In the smallest dendrimer with only four chromophores, delayed annihilation was not present, since the direct annihilation process was more efficient than the two-step delayed annihilation process. Along with an increase in the dendrimer size, the chances of originally exciting two neighboring chromophores decreased, thereby making the delayed annihilation process becomes more visible.

The change in energy hopping time is brought about by a more favorable orientation of the chromophore dipoles and/or a small decrease in the chromophore−chromophore distance due to a larger flexibility of the dendrimer. In the smaller dendrimers, direct annihilation suppresses contributions from delayed annihilation. Consequently, this study demonstrates how the energy hopping and thereby the overall annihilation can be improved by adding one additional carbon to the connecting chain. This in turn makes the x-G*n*P*r* dendrimers promising candidates as artificial light-harvesting antennas to be utilized in artificial photosynthesis.

Acknowledgment. Financial support from the Swedish Research Council, the Swedish Energy Agency, and the Knut and Alice Wallenberg Foundation is gratefully acknowledged. We further thank the Australian Research Council for a Discovery Research Grant (DP0208776) to Professor M. J. Crossley.

References and Notes

(1) Jansen, J. F. G. A.; de Brabander-van den Berg, E. M. M.; Meijer, E. W. *Science* **1994**, *266*, 1226.
(2) Vögtle, F.; Gestermann, S.; Kauffmann, C.; Ceroni, P.; Vicinelli, V.; Balzani, V. *J. Am. Chem. Soc.* **2000**, *122*, 10398.
(3) Brousmiche, D. W.; Serin, J. M.; Fréchet, J. M. J.; He, G. S.; Lin, T. C.; Chung, S. J.; Prasad, P. N. *J. Am. Chem. Soc.* **2003**, *125*, 1448.
(4) Ghaddar, T. H.; Wishart, J. F.; Thompson, D. W.; Whitesell, J. K.; Fox, M. A. *J. Am. Chem. Soc.* **2002**, *124*, 8285.
(5) Twyman, L. J.; Beezer, A. E.; Esfand, R.; Hardy, M. J.; Mitchell, J. C. *Tetrahedron Lett.* **1999**, *40*, 1743.
(6) Betley, T. A.; Holl, M. M. B.; Orr, B. G.; Swanson, D. R.; Tomalia, D. A.; Baker, J. R. *Langmuir* **2001**, *17*, 2768.
(7) Bielinska, A.; Kukowska-Latallo, J. F.; Johnson, J.; Tomalia, D. A.; Baker, J. R. *Nucleic Acids Res.* **1996**, *24*, 2176.
(8) Ottaviani, M. F.; Sacchi, B.; Turro, N. J.; Chen, W.; Jockusch, S.; Tomalia, D. A. *Macromolecules* **1999**, *32*, 2275.
(9) Roberts, J. C.; Bhalgat, M. K.; Zera, R. T. *J. Biomed. Mater. Res.* **1996**, *30*, 53.
(10) Singh, P. *Bioconjugate Chem.* **1998**, *9*, 54.
(11) Tomalia, D. A. *Sci. Am.* **1995**, *272*, 62.
(12) Pollak, K. W.; Leon, J. W.; Fréchet, J. M. J.; Maskus, M.; Abruña, H. D. *Chem. Mater.* **1998**, *10*, 30.
(13) Matthews, O. A.; Shipway, A. N.; Stoddart, J. F. *Prog. Polym. Sci.* **1998**, *23*, 1.
(14) Bar-Haim, A.; Klafter, J.; Kopelman, R. *J. Am. Chem. Soc.* **1997**, *119*, 6197.
(15) Bar-Haim, A.; Klafter, J. *J. Phys. Chem. B* **1998**, *102*, 1662.
(16) Andersson, J.; Puntoriero, F.; Serroni, S.; Yartsev, A.; Pascher, T.; Polívka, T.; Campagna, S.; Sundström, V. *Faraday Discuss.* **2004**, *127*, 295.
(17) Andersson, J.; Puntoriero, F.; Serroni, S.; Yartsev, A.; Pascher, T.; Polívka, T.; Campagna, S.; Sundström, V. *Chem. Phys. Lett.* **2004**, *386*, 336.
(18) Balzani, V.; Campagna, S.; Denti, G.; Juris, A.; Serroni, S.; Venturi, M. *Acc. Chem. Res.* **1998**, *31*, 26.
(19) Varnavski, O.; Samuel, I. D. W.; Pålsson, L. O.; Beavington, R.; Burn, P. L.; Goodson, T. *J. Chem. Phys.* **2002**, *116*, 8893.
(20) Vosch, T.; Cotlet, M.; Hofkens, J.; Van der Biest, K.; Lor, M.; Weston, K.; Tinnefeld, P.; Sauer, M.; Latterini, L.; Müllen, K.; De Schryver, F. C. *J. Phys. Chem. A* **2003**, *107*, 6920.
(21) Wang, B. B.; Zhang, X.; Jia, X. R.; Luo, Y. F.; Sun, Z.; Yang, L.; Ji, Y.; Wei, Y. *Polymer* **2004**, *45*, 8395.
(22) Choi, M. S.; Aida, T.; Yamazaki, T.; Yamazaki, I. *Chem.—Eur. J.* **2002**, *8*, 2668.
(23) De Belder, G.; Jordens, S.; Lor, M.; Schweitzer, G.; De, R.; Weil, T.; Herrmann, A.; Wiesler, U. K.; Müllen, K.; De Schryver, F. C. *J. Photochem. Photobiol., A* **2001**, *145*, 61.
(24) Karni, Y.; Jordens, S.; De Belder, G.; Schweitzer, G.; Hofkens, J.; Gensch, T.; Maus, M.; De Schryver, F. C.; Hermann, A.; Müllen, K. *Chem. Phys. Lett.* **1999**, *310*, 73.
(25) Karni, Y.; Jordens, S.; De Belder, G.; Hofkens, J.; Schweitzer, G.; De Schryver, F. C.; Herrmann, A.; Müllen, K. *J. Phys. Chem. B* **1999**, *103*, 9378.
(26) Lor, M.; Thielemans, J.; Viaene, L.; Cotlet, M.; Hofkens, J.; Weil, T.; Hampel, C.; Müllen, K.; Verhoeven, J. W.; Van der Auweraer, M.; De Schryver, F. C. *J. Am. Chem. Soc.* **2002**, *124*, 9918.
(27) Fleming, C. N.; Maxwell, K. A.; DeSimone, J. M.; Meyer, T. J.; Papanikolas, J. M. *J. Am. Chem. Soc.* **2001**, *123*, 10336.
(28) Cotlet, M.; Vosch, T.; Habuchi, S.; Weil, T.; Müllen, K.; Hofkens, J.; De Schryver, F. *J. Am. Chem. Soc.* **2005**, *127*, 9760.
(29) Flamigni, L.; Talarico, A. M.; Ventura, B.; Sooambar, C.; Solladie, N. *Eur. J. Inorg. Chem.* **2006**, 2155.
(30) Hania, P. R.; Heijs, D. J.; Bowden, T.; Pugzlys, A.; van Esch, J.; Knoester, J.; Duppen, K. *J. Phys. Chem. B* **2004**, *108*, 71.
(31) Rubtsov, I. V.; Kobuke, Y.; Miyaji, H.; Yoshihara, K. *Chem. Phys. Lett.* **1999**, *308*, 323.
(32) Sirish, M.; Maiya, B. G. *J. Photochem. Photobiol., A* **1995**, *85*, 127.
(33) Taniguchi, M.; Ra, D.; Kirmaier, C.; Hindin, E.; Schwartz, J. K.; Diers, J. R.; Knox, R. S.; Bocian, D. F.; Lindsey, J. S.; Holten, D. *J. Am. Chem. Soc.* **2003**, *125*, 13461.
(34) Lor, M.; De, R.; Jordens, S.; De Belder, G.; Schweitzer, G.; Cotlet, M.; Hofkens, J.; Weil, T.; Herrmann, A.; Müllen, K.; Van der Auweraer, M.; De Schryver, F. C. *J. Phys. Chem. A* **2002**, *106*, 2083.

(35) Lor, M.; Viaene, L.; Pilot, R.; Fron, E.; Jordens, S.; Schweitzer, G.; Weil, T.; Müllen, K.; Verhoeven, J. W.; Van der Auweraer, M.; De Schryver, F. C. *J. Phys. Chem. B* **2004**, *108*, 10721.

(36) Maus, M.; De, R.; Lor, M.; Weil, T.; Mitra, S.; Wiesler, U. M.; Herrmann, A.; Hofkens, J.; Vosch, T.; Müllen, K.; De Schryver, F. C. *J. Am. Chem. Soc*. **2001**, *123*, 7668.

(37) Maus, M.; Mitra, S.; Lor, M.; Hofkens, J.; Weil, T.; Herrmann, A.; Müllen, K.; De Schryver, F. C. *J. Phys. Chem. A* **2001**, *105*, 3961.

(38) Schweitzer, G.; Gronheid, R.; Jordens, S.; Lor, M.; De Belder, G.; Weil, T.; Reuther, E.; Müllen, K.; De Schryver, F. C. *J. Phys. Chem. A* **2003**, *107*, 3199.

(39) Atas, E.; Peng, Z. H.; Kleiman, V. D. *J. Phys. Chem. B* **2005**, *109*, 13553.

(40) Yatskou, M. M.; Koehorst, R. B. M.; van Hoek, A.; Donker, H.; Schaafsma, T. J. *J. Phys. Chem. A* **2001**, *105*, 11432.

(41) Yeow, E. K. L.; Ghiggino, K. P.; Reek, J. N. H.; Crossley, M. J.; Bosman, A. W.; Schenning, A. P. H. J.; Meijer, E. W. *J. Phys. Chem. B* **2000**, *104*, 2596.

(42) Yeow, E. K. L.; Sintic, P. J.; Cabral, N. M.; Reek, J. N. H.; Crossley, M. J.; Ghiggino, K. P. *Phys. Chem. Chem. Phys.* **2000**, *2*, 4281.

(43) Hofkens, J.; Latterini, L.; De Belder, G.; Gensch, T.; Maus, M.; Vosch, T.; Karni, Y.; Schweitzer, G.; De Schryver, F. C.; Hermann, A.; Müllen, K. *Chem. Phys. Lett.* **1999**, *304*, 1.

(44) Melinger, J. S.; Pan, Y. C.; Kleiman, V. D.; Peng, Z. H.; Davis, B. L.; McMorrow, D.; Lu, M. *J. Am. Chem. Soc.* **2002**, *124*, 12002.

(45) Ortiz, W.; Krueger, B. P.; Kleiman, V. D.; Krause, J. L.; Roitberg, A. E. *J. Phys. Chem. B* **2005**, *109*, 11512.

(46) Kilin, D.; Kleinekathofer, U.; Schreiber, M. *J. Phys. Chem. A* **2000**, *104*, 5413.

(47) Kim, D.; Osuka, A. *Acc. Chem. Res.* **2004**, *37*, 735.

(48) De Schryver, F. C.; Vosch, T.; Cotlet, M.; Van der Auweraer, M.; Müllen, K.; Hofkens, J. *Acc. Chem. Res.* **2005**, *38*, 514.

(49) Hofkens, J.; Cotlet, M.; Vosch, T.; Tinnefeld, P.; Weston, K. D.; Ego, C.; Grimsdale, A.; Müllen, K.; Beljonne, D.; Bredas, J. L.; Jordens, S.; Schweitzer, G.; Sauer, M.; De Schryver, F. *Proc. Natl. Acad. Sci. U.S.A.* **2003**, *100*, 13146.

(50) Förster, T. *Z. Naturforsch., B: Chem. Sci.* **1947**, *2*, 174.

(51) Scholes, G. D.; Fleming, G. R. *J. Phys. Chem. B* **2000**, *104*, 1854.

(52) Larsen, J.; Andersson, J.; Polívka, T.; Sly, J.; Crossley, M. J.; Sundström, V.; Åkesson, E. *Chem. Phys. Lett.* **2005**, *403*, 205.

(53) Larsen, J.; Brüggemann, B.; Polívka, T.; Sundström, V.; Åkesson, E.; Sly, J.; Crossley, M. J. *J. Phys. Chem. A* **2005**, *109*, 10654.

(54) Larsen, J.; Brüggemann, B.; Sly, J.; Crossley, M. J.; Sundström, V.; Åkesson, E. *Chem. Phys. Lett.* **2006**, *433*, 159.

(55) Sly, J. Ph. D. Thesis, The University of Sydney, 2004.

(56) Khoury, T. Ph. D. Thesis, The University of Sydney, 2006.

(57) Hogan, C. F.; Harris, A. R.; Bond, A. M.; Sly, J.; Crossley, M. J. *Phys. Chem. Chem. Phys.* **2006**, *8*, 2058.

(58) Rogers, J. E.; Nguyen, K. A.; Hufnagle, D. C.; McLean, D. G.; Su, W. J.; Gossett, K. M.; Burke, A. R.; Vinogradov, S. A.; Pachter, R.; Fleitz, P. A. *J. Phys. Chem. A* **2003**, *107*, 11331.

(59) van Amerongen, H.; Valkunas, L.; van Grondelle, R. *Photosynthetic Excitons*; World Scientific Publishing Co. Pte. Ltd: Singapore, 2000.

(60) Scholes, G. D. *Annu. Rev. Phys. Chem.* **2003**, *54*, 57.